Molecular Vision 2002; 8:341-50 <http://www.molvis.org/molvis/v8/a41>
Received 10 June 2002 | Accepted 5 September 2002 | Published 15 September 2002

p53 regulates apoptotic retinal ganglion cell death induced by N-methyl-D-aspartate

Yan Li,[1] Cassandra L. Schlamp,[1] Gretchen L. Poulsen,[1] Mark W. Jackson,[2] Anne E. Griep,[2] Robert W. Nickells[1,3]

Departments of [1]Ophthalmology and Visual Sciences, [2]Anatomy, and [3]Physiology, University of Wisconsin Medical School, Madison, WI

Purpose: The tumor suppressor protein p53 plays a central role in regulating apoptosis in a variety of neuronal cell types. Previous studies have indicated that retinal ganglion cell (RGC) death induced by ischemia follows a p53-dependent pathway. Ischemia causes wide-spread damage to the retina, eliciting multiple different damaging pathways. We conducted experiments to specifically investigate the role of p53 in RGC death activated by overstimulation of the N-methyl-D-aspartate (NMDA) receptor, an ionotropic glutamate dependent calcium channel normally involved in glutamate neurotransduction.

Methods: RGC death was induced in both wild-type (CB6F1 or 129/Sv) and p53-deficient (129/Sv background) mice by a single intravitreal injection of either 40 or 160 nmol of NMDA into one eye leaving the other eye as an untreated control. Cell loss was quantified by comparing the number of surviving cells in the retinas from experimental eyes relative to the control eyes of the same animals. The accumulation of p53 mRNA in retinas was monitored by reverse-transcription PCR (RT-PCR) of retinal total RNA isolated from mice injected with 40 nmol of NMDA. The functional requirement for p53 was monitored in p53-deficient mice after intravitreal injection of 160 nmol of NMDA. Immunohistochemistry for cleaved poly(ADP-ribose) polymerase (PARP) was performed on p53-deficient mice after intravitreal injection of 160 nmol of NMDA.

Results: In wild-type CB6F1 mice, p53 mRNA levels are elevated within 3 h after NMDA injection. This accumulation correlates with the onset of changes in RGC nuclear morphology that precedes pyknosis, which occurs by 6 h. Mice (129/Sv) deficient for one or both alleles of p53 show no developmental change in RGC number, compared to wild-type animals (Mann-Whitney test, $p=0.824$), suggesting that p53 is not required for developmental programmed cell death of RGCs. In adult mice, however, p53-dependent changes in the rate of RGC death after exposure to 160 nmol of NMDA were observed. Four days after injection, p53+/+ and p53-/- mice exhibit statistically equivalent amounts of cell loss ($p>0.1$), while p53+/- mice have significantly attenuated cell loss ($p<0.002$), relative to the other groups. RGCs from NMDA-treated p53+/+ and p53-/- mice were analyzed further using immunohistochemistry to identify the cleavage products of poly(ADP-ribose) polymerase (PARP), a known substrate for caspases. Cleaved PARP was found in p53+/+ and p53+/- eyes, but not in p53-/- mice.

Conclusions: Developmental RGC programmed cell death does not require p53. Selective overstimulation of the glutamate-dependent NMDA-receptor in adult mice activates a p53-dependent pathway of death in RGCs. The requirement for p53 is not absolute, however, because mice lacking this gene are able to execute an alternative pathway of cell death. Examination of the cleavage of PARP, which is a substrate for caspases, suggests that the p53-dependent pathway utilizes these proteases, but the p53-independent pathway does not.

Ischemia affects all cell types of the retina [1,2]. Growing evidence suggests that the effects of ischemia on the inner retina, which, includes the retinal ganglion cells (RGCs) and the inner nuclear layer, is mediated by abnormally high levels of the excitatory amino acid glutamate [3-6]. Glutamate is the predominant neurotransmitter of the central nervous system. It interacts with numerous receptor sub-types, which fall into two major classes: those coupled to G-proteins (metabotropic) and those connected directly to transmembrane channels (ionotropic). The toxic effects of elevated levels of glutamate are predominantly mediated by the overstimulation of ionotropic receptors. Overstimulation of the class of these receptors that respond specifically to the glutamate analog N-methyl-D-aspartate (NMDA) leads to an overload of intracellular Ca^{2+}. Such elevations in Ca^{2+} elicit various cytotoxic biochemical reactions including the activation of nitric oxide synthase and the generation of reactive *NO free radicals [7]. Two other classes of ionotropic receptors, which respond to the agonists kainate and α-amino-3-hydroxy-5-methyl-4-isoxazolepropianate (AMPA), respectively, can also mediate Ca^{2+} overload when overstimulated, but they are somewhat less permeable to this ion than the NMDA receptor. This preferential permeability to calcium ions has established the NMDA receptor as the primary mediator of glutamate neurotoxicity [7].

RGCs are highly sensitive to the toxic effects of elevated glutamate, but the mechanism of how this response is mediated is not clear. NMDA receptors are abundant on RGCs and

Correspondence to: Dr. Robert W. Nickells, Department of Ophthalmology and Visual Science, 6640 Medical Science Center, University of Wisconsin, 1300 University Ave, Madison, WI, 53706; Phone: (608) 265-6037; FAX: (608) 262-0479; email: nickells@facstaff.wisc.edu

a sub-population of cells in the inner nuclear layer, presumed to be amacrine cells [8] and both these cell types are sensitive to the toxic effects of NMDA [9]. In addition, drugs that block the NMDA receptor channel and limit Ca^{2+} influx, attenuate the degeneration of the inner retina after short periods of ischemia caused by extreme transient elevations in intraocular pressure [5]. Other studies, however, suggest that AMPA-kainate receptors also play an important role in the death of RGCs under a variety of damaging conditions [10-12]. Whatever the mechanism, elevated glutamate levels may play an important role in the pathology of several eye diseases including ischemia, optic nerve damage and glaucoma [5,13,14].

After hyperstimulation of one or more of the glutamate receptors, the mechanism of neuronal death induced by excitotoxins is complex. Several studies indicate that both apoptotic and necrotic pathways of cell death can be activated [15-20] depending on the severity of exposure to an excitatory amino acid [18] and which of the ionotropic receptors is activated [21]. Necrotic episodes of cell death are drastic, often associated with cellular swelling and rupture leading to inflammation. Apoptosis is a less dramatic pathway of cell death to the whole organism. The dying cell executes its own intrinsic genetic program that regulates the breakdown and subsequent removal of cellular debris before it can adversely affect surrounding tissues. There are several key proteins involved in this process, including the tumor suppressor p53, which is involved in the early steps of the pathway [22,23]. The p53 protein acts as a direct transcriptional activator of the Bax gene [24], which in turn, modulates many of the downstream factors commonly associated with apoptosis [25,26], including the activation of cysteine-proteases called caspases that systematically digest the contents of the cell [27-29].

The possible functional role of p53 in glutamate-induced neuronal apoptosis has recently drawn attention [20]. Inactivation of the p53 gene, or reduced p53 expression, protects cells from the excitotoxin kainate and focal ischemic damage [30,31]. In the retina, apoptosis induced by retinal ischemia in rats is associated with increased expression of p53 mRNA [5] and mice with reduced expression of p53 show resistance to ischemia-induced RGC death confirming a functional role for this protein [32]. However, because the effects of ischemia may be several fold, including the activation of several different glutamate receptors, it is not clear what event signals the activation of p53-dependent RGC death. In order to clarify this, we used NMDA to specifically activate RGC death by overstimulation of this receptor. The results reported here indicate that NMDA-stimulated RGC death occurs through a p53-dependent pathway in cells carrying functional alleles of this gene. The p53-dependent pathway results in the activation of at least some members of the caspase protease cascade. NMDA also stimulates cell death in p53-deficient RGCs, however, but these cells appear to utilize an undefined caspase-independent cell death pathway.

METHODS

Experimental animals: The mice used in this study were handled in accordance with the Association for Research in Vision and Ophthalmology resolution for the use of animals in research. Mice containing targeted loss-of-function alleles of p53 were generated by homologous recombination as described [33]. The mutant alleles were carried in animals with a 129/Sv genetic background. Heterozygotes were bred to generate offspring that contain two functional alleles of p53 (p53+/+), one functional allele (p53+/-), and no functional alleles (p53-/-). The genotypes of mating pairs and all offspring were confirmed by PCR analysis of DNA isolated from tail biopsies. Reverse transcriptase-PCR (RT-PCR) experiments were conducted on CB6F1 mice.

Axon counting of optic nerves: Optic nerves of sacrificed p53-deficient mice were fixed overnight at 4 °C in 2.5% (wt/vol) glutaraldehyde in 100 mM phosphate buffered saline (pH 7.4, PBS), embedded in JB-4 plastic (glycol methacrylate; Polyscience, Warrington, PA), and sectioned at 2 μm thickness. Cross sections were stained using a silver nitrate impregnation technique, which selectively stains the axons [34]. Stained sections were digitized using an Olympus BH-2 photomicroscope (Mellville, NY) attached to a Sony 3-chip CCD video camera (Sony, New York, NY) with direct electronic feed into a Gateway 2000 personal computer (North Sioux City, SD). The area of each optic nerve was measured and the number of axons in 10 regions of each nerve was counted using Optimas imaging software (Media Cyberretics LP, Bothell, WA). The total number of axons counted per nerve ranged from 2.7% to 5% of the entire nerve. These values were then used to extrapolate the total number of axons in each nerve. This was repeated for three sections of each nerve and then the totals were averaged for each mouse. Four mice of each genotype were counted.

NMDA injection: Intravitreal NMDA injection was performed as described previously [9]. Two μl of either a 20 mM or 80 mM solution of NMDA in balanced saline solution (BSS) was injected into the vitreous of the right eye of each mouse, which delivered a dose of either 40 or 160 nmol of NMDA, respectively. The left eyes were not injected and served as untreated controls. In other control experiments, right eyes were injected with BSS alone, which did not cause cell death, as previously reported [9].

Quantification of cell loss in the ganglion cell layer (GCL): Cell loss in the GCL was determined as described before [9]. Thick longitudinal sections (2 μm) through the entire retina were stained with the DNA-specific fluorescent dye, 4,6-Diamidino-2-phenylindole (DAPI; Roche Molecular Biochemicals, Indianapolis, IN) to identify nuclei. Sections were viewed using a Zeiss Axiophot fluorescent microscope (Thornwood, NY). The total number of cells in the GCL was counted in sections of 400 μm of peripheral and central retina in the superior half of each eye (both experimental and control of each mouse) and normalized to the number of photoreceptor nuclei in the same section. At least 4 sections were counted for each eye evaluated. The percentage of cells remaining in the GCL from the NMDA-injected eye was calculated by comparing it to the control eye from the same mouse.

Reverse Transcriptase PCR (RT-PCR) analysis of p53 mRNA abundance: RT-PCR was used to estimate p53 mRNA

abundance in retinas of NMDA injected eyes. CB6F1 mice were injected with 40 nmol of NMDA and sacrificed 1, 3, 6, 18, 24, and 48 h after injection. To determine the earliest stage of effect on the ganglion cell layer, we initially fixed the retinas, prepared flat-mounts, and stained them with cresyl violet to highlight both the Nissl-substance found in RGCs and the nuclear morphology of all the cells in this layer. Stained retinas then were examined under bright field microscopy to determine the window of time after NMDA injection when the RGCs begin to show the first stages of nuclear condensation characteristic of cell death. After this window was determined, different mice were injected and the retinas harvested before, during, and after this critical window. Four retinas (experimental or control) were pooled for each time point and snap frozen. Total RNA was isolated using the Tri-Reagent protocol (Molecular Research Center, Inc., Cincinnati, OH), which is based on the method of Chomczynski [35]. First strand cDNA was made using oligo-dT as a primer and Moloney murine leukemia virus reverse transcriptase as described previously [36], except that the amount of cDNA synthesized in each sample was quantified by incorporating a trace amount of α-^{32}P-dCTP into the reaction. Incorporated radioactivity was measured by precipitating an aliquot of cDNA with 50 µg of cold yeast RNA in 25% ice cold trichloroacetic acid (TCA). TCA precipitated polynucleotides were trapped by filtering them onto a GF/C glass fiber filter, washing twice with 25% TCA and once with ice-cold 95% ethanol. Filters were air-dried and counted in a Beckman (Fullerton, CA) Model LS 5801 scintillation counter.

For PCR, an equal amount of cDNA (approximately 2 ng) prepared from control and experimental retinas was used as template to amplify fragments of p53 or actin cDNAs. The primers used for amplification of p53 were: forward 5'-CTCAAAAAACTTACCAGGGC and reverse 5'-CACCACGCTGTGGCGAAAAGTCTG, and for amplification of actin were: forward 5'-CTCTCCCTCACGCCATCCTG and reverse 5'-CCGCCTAGAAGCACTTGCGG. Both cDNAs were amplified using PCR conditions of 3 cycles at 94 °C (45 s), 40 °C (2 min), 72 °C (2 min) followed by 35 cycles at 94 °C (45 s), 55 °C (1 min), 72 °C (2 min). PCR reactions were analyzed on 1% agarose gels. To increase specificity of p53 analysis, gels were alkaline blotted to MagnaCharge nylon membrane (Fisher Scientific, Hanover Park, IL) and probed with a fragment of mouse p53 cDNA labeled with digoxygenin (Roche Molecular Biochemicals). Bands for p53 on the nylon membrane were detected by reacting the membrane with anti-digoxigenin antibodies conjugated to alkaline phosphatase, developing it with CDP-Star (Roche Molecular Biochemicals) and exposing it to X-OMAT AR X-ray film (Kodak, Rochester, NY). Images of both the ethidium bromide-stained agarose gels (for actin) and the X-ray film exposures (for p53) were digitized on a Hewlit Packard ScanJet IIcx flatbed scanner (Palo Alto, CA) and used for quantification by NIH Image (v1.57). Band densities for p53 in samples were first normalized to the actin bands in each sample and then compared between the control and experimental eyes for each time point.

To confirm RT-PCR results, two independent experiments were also analyzed by real time PCR. Samples were prepared from total RNA as described above and PCR reactions were identical except that fluorescein and SYBR green was also included in each reaction and the second cycling program was extended from 35 cycles to 45 cycles to ensure that all reactions had reached the plateau stage of the amplification. The PCR reactions were run in a BioRad iCycler (BioRad, Richmond, CA). All samples were first adjusted to yield identical threshold crossing (Tc) levels for actin cDNA fragments. The synthesis of primer-dimers was controlled for by running reactions with either no template or nonspecific template (human first strand cDNA). Primer-dimer formation did occur in these samples, but exhibited a Tc level an order of magnitude below the Tc of target molecules.

Immunohistochemistry for cleaved Poly(ADP-ribose) Polymerase (PARP): Wild-type or p53-deficient mice were injected with 160 nmol of NMDA and sacrificed after two days, when cell loss ranged from 40-50% of the cells in the GCL of mice with the 129/Sv genetic background. The eyes were fixed as whole globes in 4% paraformaldehyde in phosphate buffer for 1 h at 22 °C followed by overnight in 0.4% paraformaldehyde at 4 °C. The anterior chamber and lens was then dissected away and the remaining eye cup was embedded in paraffin and sectioned at 5 µm. Sections were affixed to glass Plus slides (Fisher Scientific) and then microwaved for 8 min at 50% power for antigen retrieval. Deparaffinized sections were washed in PBS, blocked overnight in 4% bovine serum albumin in PBS at 4 °C, and then incubated in PBS containing a 1:200 dilution of a polyclonal antiserum to the p85 fragment of cleaved PARP (Promega, Madison, WI) overnight at 4 °C. After incubation in the primary antibody, the slides were washed and incubated further with a goat anti-rabbit IgG conjugated to horse-radish peroxidase. Reacting antibodies were detected with an ABC kit (Vector Elite System, Burlingame, CA) and diaminobenzidine. Stained retinal sections were imaged using a Zeiss Axiophot Microscope with Nomarski optics. Non-specific antibody reactions were controlled by staining sections from control and experimental eyes of mice from all three p53 genotypes and by staining positively-reacting sections without primary or secondary antibodies.

Identification and Evaluation of Apoptotic Cells: Dying cells were identified using standard histological and histochemical methods. Cells undergoing DNA fragmentation were stained in paraffin-embedded sections of retinas using the TUNEL protocol [9,37]. Histological evaluation of nuclei in dying cells was made from either DAPI-stained or toluidine blue-stained sections of retinas embedded in JB-4 Plus or cresyl violet-stained retinal whole-mounts.

Statistical Evaluation: Data are represented as mean plus or minus standard deviation. A Mann Whitney test was used to evaluate cell count data from mice with different complements of the wild-type p53 gene, while a Wilcoxon paired-sample test was used to evaluate the increase in p53 PCR product between injected and control eyes.

RESULTS

Programmed cell death of RGCs during development is p53-independent: Mice typically lose 50% of the number of RGCs during developmental remodeling of the retina in the first two weeks of postnatal life. To measure the effects of p53 during developmental programmed cell death, optic nerve sections from adult (>1 month old) mice carrying 0, 1, or 2 functional p53 alleles were stained by the Bielschowsky method of silver impregnation to distinguish axons. Axon numbers were counted on sections from 4 mice of each group. No statistical difference was observed (Mann-Whitney test, p=0.824; Table 1). TUNEL-staining of retinas of mice between 4 and 14 days of age showed elevated levels of dying cells in the GCL between 7 and 10 days in all 3 genotypes examined (data not shown).

p53 mRNA accumulation coincides with NMDA-induced cell death: CB6F1 mice were injected intravitreally with 40 nmol of NMDA. Cresyl violet-staining of retinal whole-mounts from these mice showed that changes in nuclear morphology were detected in some cells as early as 1 h, with the majority of cells exhibiting early stages of chromatin condensation by 3 h post-injection (Figure 1). By 6 h, the majority of cells in this layer had fully condensed nuclei and by 18 h most of these had become fragmented or were lost as the debris of the dead cells was cleared. Analysis of p53 mRNA levels was chosen during the time window of 1-6 h to coincide with this period of nuclear changes.

RT-PCR analysis of p53 mRNA was conducted on retinal RNA samples harvested at 1, 3, and 6 h after NMDA injection. The amount of PCR amplified cDNA for p53 was normalized to a control cDNA in each sample (actin) and used to estimate the relative abundance of p53 mRNA present. Nearly all control retina samples had low levels of p53 cDNA. No increase in cDNA quantity was detected in experimental retinas 1 h after NMDA treatment, but a small decrease was observed in two samples (60.5 ± 16.3% of control retina levels, two experiments (n) of four pooled retinas per sample, mean ± standard deviation). Retinas harvested 3 h after injection showed a signficant increase in the p53 PCR product relative to control retinas (169.2 ± 47%, n=5, p=0.05, Wilcoxon paired-sample test). Retinas harvested 6 h after injection showed in-

Table 1. Axon counts from murine optic nerves

Mouse Genotype	Axon Counts (Total ± SD)
p53+/+	55381 ± 3920
p53+/-	54359 ± 8859
p53-/-	57433 ± 3767

Axon counts from optic nerves of mice with different backgrounds for p53. Each count represents the average (with standard deviation) of four nerves from eyes of each background and is an accurate indicator of the number of ganglion cells in the eyes of these mice. Cell number is not affected by the loss of functional alleles of p53 indicating that this gene does not regulate developmental programmed cell death of the RGCs in the developing retina.

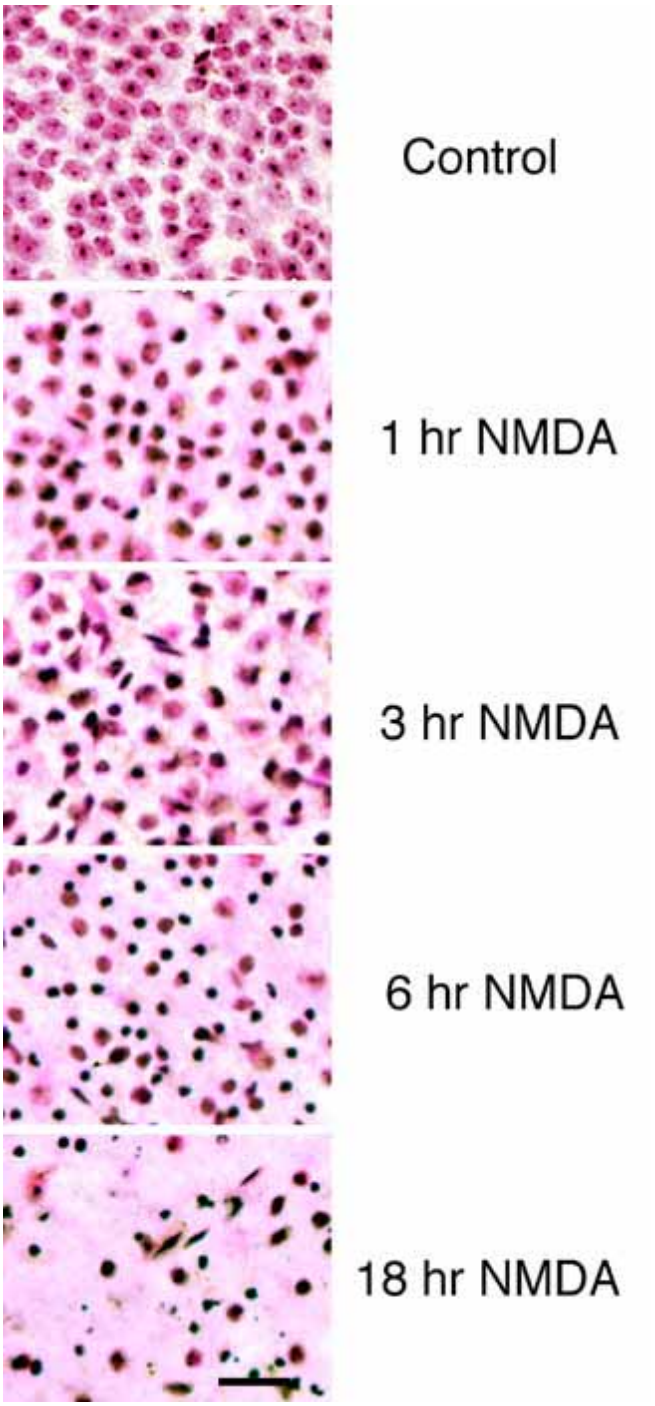

Figure 1. Effect of NMDA on nuclear morphology in the ganglion cell layer. Changes in nuclear morphology are rapidly observed in cells of the ganglion cell layer after intravitreal injection of NMDA. Shown are Nissl-stained wholemounts of mouse retinas harvested at 1, 3, 6, and 18 h after intravitreal injection of 40 nmol of NMDA. At 1 h, several cells in the ganglion cell layer show early signs of changes in nuclear morphology, suggestive of early stages of chromatin condensation. By 3 h, nearly all the presumed RGCs have this appearance or have become pyknotic. All these cells are pyknotic by 6 h. After 18 h, few cells remain. For the most part, these remaining cells and their nuclei have become fragmented and appear to be in the final stages of death. Size bar represents 35 μm.

consistent changes in p53 cDNA levels, ranging from a 40% increase to a 54% decrease in p53 cDNA relative to control eyes (Figure 2).

Real time PCR confirmed data collected by RT-PCR analysis. Two experiments were performed and analyzed by real time PCR (Table 2). In each case, p53 cDNA levels were elevated in retinal samples collected 3 h after NMDA injection, although the increases were generally larger than detected by RT-PCR. Real time analysis also indicated that p53 cDNA levels appeared to transiently decrease 1 h after NMDA injection and exhibit variable levels at 6 h after injection.

NMDA-induced RGC death occurs by p53-dependent and independent pathways: The contribution of p53 to NMDA-induced cell death was evaluated by analyzing the cell loss in the GCL in mice carrying mutant alleles of p53 after intravitreal injection of 160 nmol of NMDA. Representative micrographs of DAPI-stained sections of central retinas from a mouse of each genotype are shown in Figure 3. Cell loss was quantified in mice sacrificed 4 days after injection, at a time when nearly complete ganglion cell loss is expected in wild-type animals [9]. Mice from each genotype showed evidence of cell loss (Figure 4). There was no significant difference in cell loss between the p53+/+ and p53-/- mice (Mann-Whitney test, $p>0.1$). Mice heterozygous for the mutant p53 allele, however, showed significantly reduced cell loss ($p<0.02$), relative to the other two groups.

Table 2. Real time PCR measurements of retinal p53 mRNA levels

Sample	Experiment 1	Experiment 2
1 h	ND	-29.7 fold
3 h	16.56 fold	13.36 fold
6 h	-1.06 fold	-1.82 fold
18 h	ND	-4.22 fold

Real time PCR results demonstrating that p53 mRNA levels are elevated in retinas 3 h after NMDA injection into the eye. The values indicating a difference in p53 cDNA levels were calculated by taking 2 to the exponential of the value of the threshold crossing difference between the experimental and control eyes at each time point. The values are presented as fold differences. ND, not determined.

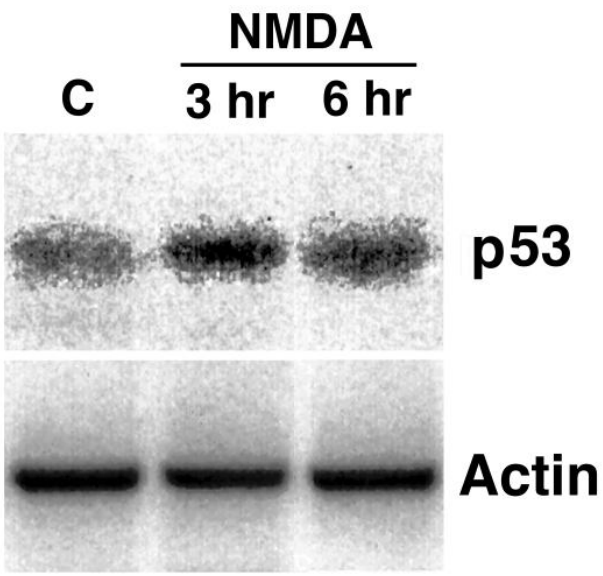

Figure 2. Upregulation of p53 expression coincides with early cell death. The upregulation of p53 expression coincides with the period of early cell death. **Top Panel**: p53 message levels were measured by RT-PCR analysis followed by Southern blot analysis using a murine p53 probe. Shown is an autoradiograph of a representative blot. **Lower Panel**: Actin message levels in the same samples were measured by RT-PCR and the products detected by staining with ethidium bromide. Shown is a negative image of a representative ethidium bromide-stained gel. The level of p53 was quantified as described in the Methods. Elevated levels of the p53 cDNA fragment are consistently observed in the retinas 3 h after NMDA injections.

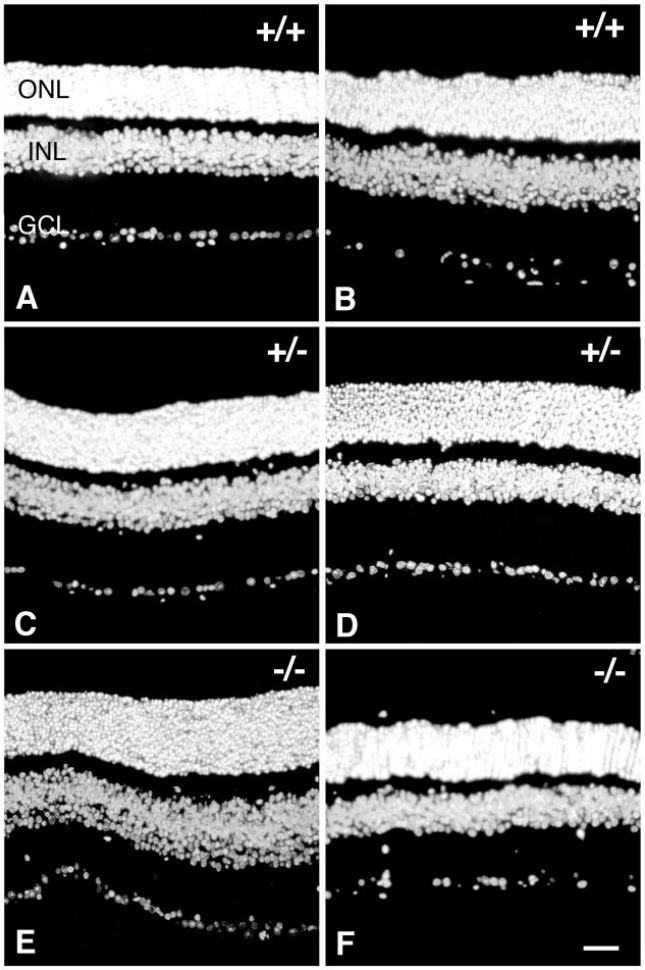

Figure 3. NMDA-induced cell loss is attenuated in p53+/- mice. NMDA-induced cell loss is attenuated, but not blocked, in p53+/- mice. Micrographs showing DAPI-stained sections of control and NMDA-injected (160 nmol) retinas from p53+/+ (**A**, **B**), p53+/- (**C**, **D**), and p53-/- (**E**, **F**) mice. The p53 alleles were maintained on an inbred 129/Sv genetic background. The animals were sacrificed 4 days after treatment. The cell loss in the retinal ganglion cell layer (GCL) is nearly identical in p53+/+ and p53-/- mice. However, the cell loss appears to be reduced in p53+/- mice at this time point. ONL, outer nuclear layer; INL, inner nuclear layer. Size bar represents 20 μm.

Cleaved PARP is only detected in mice carrying functional alleles of p53: To determine if p53+/+ and p53-/- mice executed RGC death by alternative pathways, we examined if RGCs died with different morphological characteristics and if they expressed different apoptosis-related molecules. Dying cells in eyes after NMDA injection were evaluated by TUNEL, DAPI, and toluidine blue staining. No obvious difference in the TUNEL pattern was detected between wild-type and p53 null mice (data not shown). A comparison of nuclear morphology between the two genotypes was also unremarkable.

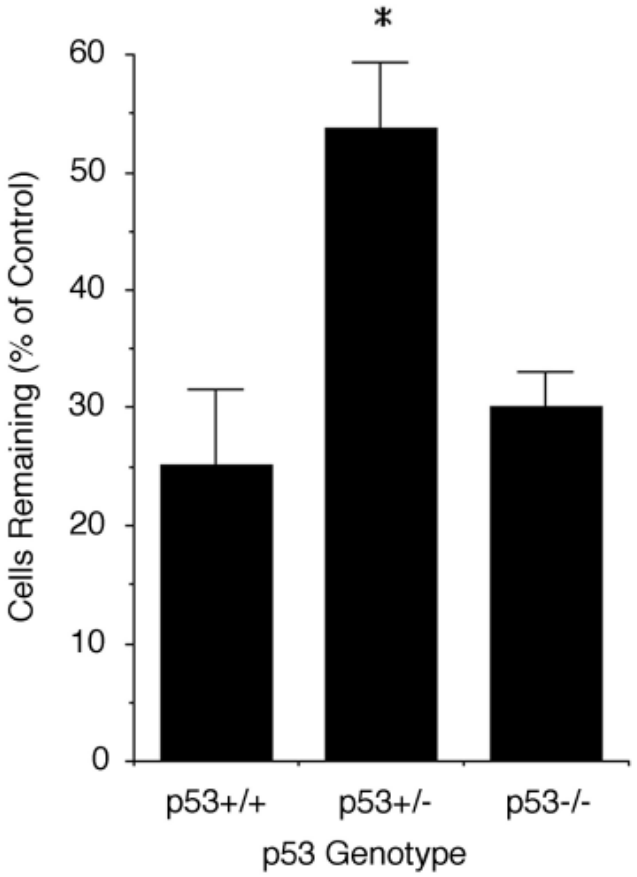

Figure 4. Quantification of NMDA-induced cell loss in p53 mutant mice. Quantitative cell loss in p53 wild-type and p53 mutant mice suggests distinct pathways of cell death. Bar graph showing quantitative analysis of cell counts in the ganglion cell layer of p53 mice 4 days after intravitreal injection of 160 nmol of NMDA. The data are represented as a percentage of cells in the control retinas that remain in the experimental eyes. The p53+/+ (an average of 74.8% cell loss, n=6) and p53-/- (an average of 70% cell loss, n=8) mice exhibit statistically equivalent amounts of cell loss (Mann-Whitney test, $p>0.1$). Previous studies using Thy-1 to identify retinal ganglion cells indicated that approximately 70% of the cells in this layer were ganglion cells (9, 26). Consequently, the amount of cell loss in these mice is probably indicative of nearly 100% ganglion cell death at this time point. Alternatively, p53+/- mice (an average of 46.3% cell loss, n=14) show significantly reduced cell loss (*$p<0.02$), relative to the other groups. The results suggest that a restricted p53-dependent pathway is active in heterozygous mice, but homozygous null animals utilize an alternative pathway.

Dying cells exhibited densely-staining "pyknotic" nuclei in the ganglion cell layer of both groups of mice (Figure 5).

Conversely, immunohistochemical staining for cleaved PARP showed a clear distinction between wild-type and p53-knockout mice. Strong staining for the p85 fragment was detected in NMDA-injected eyes of wild-type mice (Figure 6A), while more variable staining was detected in p53+/- mice (data not shown). In these latter animals, the staining was not uniform and often restricted to clusters of cells. Unlike either the p53+/+ or p53+/- animals, no PARP staining was detected in p53-/- mice (Figure 6B). No staining was detected in control eyes of any mouse examined (data not shown).

DISCUSSION

Previous studies have shown that RGC death activated by pressure-induced ischemia/reperfusion is at least partially dependent on the function of the tumor suppressor protein p53 [5,32]. These findings are consistent with numerous reports demonstrating p53-dependent cell death in neurons exposed to ischemic conditions [38-41]. Ischemia is associated with the accumulation of elevated levels of the excitatory amino acid glutamate, which can mediate toxic effects to neurons through excitation of at least 3 different receptor sub-types. Our findings extend observations in retinal ganglion cells to show that direct overstimulation of the NMDA receptor activates a p53-dependent pathway of cell death. Part of the evidence supporting this conclusion is the RT-PCR (Figure 2)

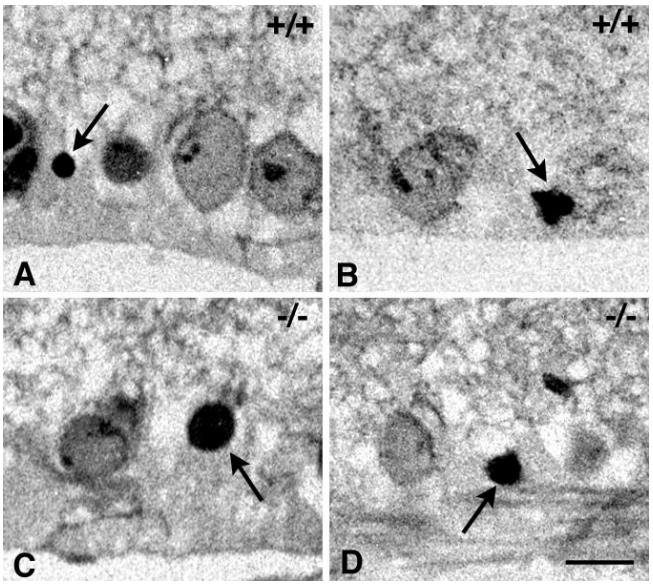

Figure 5. Histologic evaluation of the ganglion cell layer in NMDA treated p53 mutant mice. Cell death in p53 wild-type and p53-null mice is associated with the formation of pyknotic nuclei. Micrographs of toluidine blue-stained retinal sections taken 2 days after injection of 160 nmol of NMDA. **A**, **B**: Close-up of the ganglion cell layer of wild-type mice showing both normal appearing and pyknotic nuclei (arrows). **C**, **D**: Close-up of the ganglion cell layer of p53-null mice showing similar pyknotic nuclei. Based on morphological criteria, these results suggest that an apoptotic-like mechanism is active in both groups of mice. Size bar represents 7 μm.

and real time PCR (Table 2) data showing that after an initial drop in p53 mRNA accumulation, these transcripts accumulate coinciding with the initial period of early cell death after exposure to NMDA. The window of p53 mRNA accumulation is brief, however, because by 6 h message levels had begun to drop below control retinal values. The loss of p53 after 3 h may reflect the loss of RGCs after this time point, but the initial loss of message is not as easily explained. It is possible that nascent p53 transcripts are lost in the early period of gene downregulation that occurs in these cells in response to damaging stimuli [25]. Accumulation of p53 after this point may be due to the active transcription of this gene.

One of the caveats of this analysis is that the real time PCR measurements show a greater increase in p53 in the 3 h samples and a greater decrease in p53 in the 1 h samples than observed by RT-PCR. The discrepancy between methods of measurement likely reflects both the difference when comparing a sensitive quantitative method with a semi-quantitative method and the low abundance of p53 transcripts in the retina. In the case of the latter, any small changes in p53 abundance would likely be reflected as large differences in relative comparisons like “percent changes” or “fold-changes”. It should be noted, however, that even with the discrepancies, both methods showed the same trend in p53 expression. In addition, these results are consistent with findings from others using immunocytochemistry on ischemic rat retinas [5].

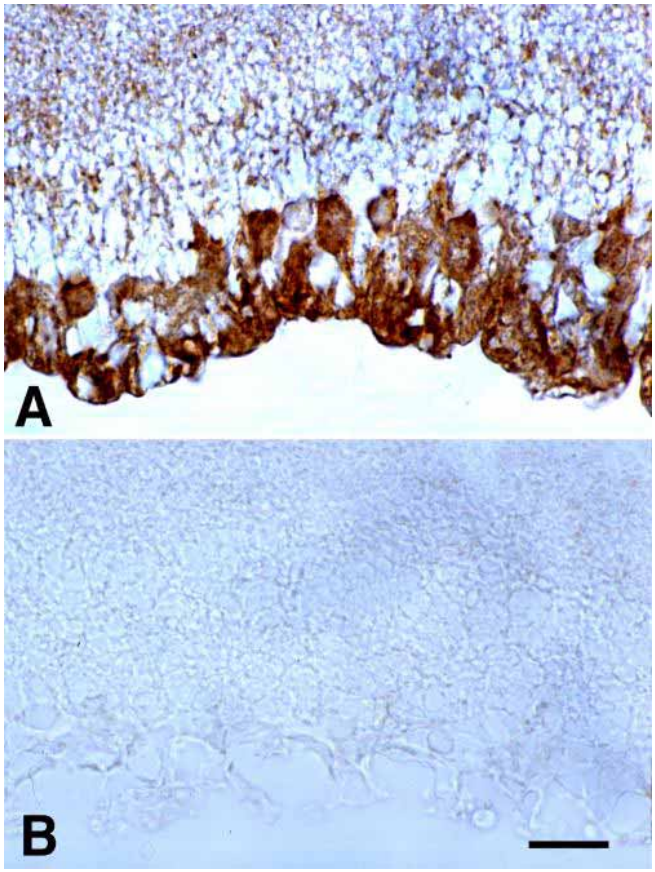

Figure 6. PARP cleavage correlates with the presence of functional alleles of p53. Immunohistochemical staining for cleaved PARP in (**A**) p53+/+ mice, and (**B**) p53-/- mice, 2 days after intravitreal injection of 160 nmol of NMDA. Positive staining of the nuclei and inner plexiform layer is restricted to mice carrying functional p53, while none of the p53-/- mice examined had any detectable staining. Positive staining for cleaved PARP was also present in p53+/- mice (data not shown), although it was less intense and variable through out the ganglion cell layer. Size bar represents 15 μm.

The strongest evidence for a role for p53 comes from experiments on mice carrying mutant alleles of this gene. Mice carrying only one functional allele of p53 show significantly reduced cell death after 4 days as compared to their p53 wild-type counterparts. We interpret this finding to suggest that the loss of one p53 allele leads to reduced production of p53 protein making these cells less efficient at activating the apoptotic program. The fact that cells still die in p53+/- mice supports this interpretation. Interestingly, mice completely deficient for p53 exhibit no decrease in RGC death as compared to p53 wild-type animals, suggesting that RGCs can die by a p53-independent mechanism in the absence of functional p53. Preliminary studies indicate that the kinetics of cell loss is slower in p53-deficient mice (data not shown), even though both p53-wild-type and p53-deficient mice exhibit maximum cell loss by 4 days.

The finding that only heterozygous mice have attenuated cell loss is not unexpected. Two independent studies of cell loss after ischemic damage to the brain [31] and retina [32] observed the same phenomenon, suggesting that neurons can die by both p53-dependent and p53-independent mechanisms when damaged by ischemia. Our results, obtained using direct exposure to the excitotoxin NMDA, are consistent with the idea that ischemia stimulates excitotoxic cell death through the activation of this glutamate receptor.

p53-dependent and p53-independent pathways of cell death: Cells can die by utilizing different molecular pathways [42] and it is clear that at least some of these pathways are not dependent on p53 [32,43-48]. It remains to be established, however, if p53-dependent and p53-independent pathways funnel into the same common latter events that are considered hallmarks of apoptosis. The examination of NMDA-induced RGC death offers a chance to address this question. Both pathways appear to execute an apoptotic-like program based on changes in nuclear morphology. A major component in many forms of cell death is the cascade of cysteine proteases known as caspases [27,28]. We used the cleavage of PARP as an estimate for caspase activity in mouse RGCs. PARP is cleaved by several caspases although it is most often recognized as a substrate for caspase 3 [49]. Exposure to NMDA causes PARP cleavage in wild-type mice, consistent with other studies in which both PARP cleavage and caspase activity is activated in these cells by damage to the optic nerve [50-53] or by retinal ischemia or excitotoxicity [6,54,55]. Although examining the cleavage of PARP places obvious limitations on our ability to conclusively judge caspase activity, the lack of staining for cleaved PARP in p53-/- RGCs suggests that the p53-independent pathway is also caspase-independent. This observation is similar to those found in studies examining the

role of another apoptotic regulatory gene. Cerebellar granule cells are susceptible to excitotoxic stimuli, where they die by a caspase-dependent mechanism that can be attenuated with caspase inhibitors [26]. If these neurons lack a functional Bax gene, which can be regulated by p53 in many cells [24] and promotes apoptotic cell death [56-59], they are still susceptible to the same excitotoxic stimuli [26], but they no longer respond to caspase inhibitors, suggesting that they are now utilizing a caspase-independent pathway of death. Not surprisingly, RGCs lacking Bax are also susceptible to excitotoxic exposure [59].

Caspases are no longer considered essential to execute the cell death pathway and recent speculation suggests that neurons in particular utilize caspase-independent pathways in order to hold a tighter regulatory control over the cell death process [42]. Additionally, several new studies indicate that caspase activity, once blocked or eliminated, can be replaced by other proteases in the cell such as members of the calpain family [60]. Calpains are abundant in the retina [61] and it is not unreasonable to speculate that RGCs damaged by excitotoxic exposure could utilize these proteases if unable to activate the caspase cascade. The mechanism of calpain activation during cell death is not clear, but these proteases are activated by free calcium [62], which is the primary result of hyperactivation of the NMDA receptor [7].

Our experiments indicate that NMDA can activate both p53-dependent and p53-independent pathways of cell death. A review of reports that document the dependence of RGC death on p53, Bax, and caspases suggests that there are at least three distinct molecular pathways active in these cells. The first pathway is active in cells undergoing developmental programmed cell death or dying in response to optic nerve crush. This pathway is both Bax- and caspase-dependent [51,52,59,63,64], but not p53-dependent (this study and data not shown), consistent with other reports that neuronal programmed cell death is unaffected in p53 null animals [43]. It is notable that cell death in both these situations is thought to originate from neurotrophin deprivation [65,66]. A second pathway is activated by NMDA and is both p53- and caspase-dependent [6,55], and may require Bax activation as well. Lastly, a third pathway that is independent of p53, Bax, and caspases is activated in RGCs by NMDA, but only when the conventional p53/Bax pathway is compromised. Studies by others [5,32] indicate that ischemia can activate both the second and third pathways of cell death. Not enough evidence is currently available to determine which pathway(s) is activated by ocular hypertension.

Lastly, the genetic background of mice may influence how much of a role p53 plays in activating neuronal cell death. In one study, for example, the number of sympathetic neurons in the superior cervical ganglia was significantly increased in p53-/- mice [67], while in another, the lack of p53 was associated with severe ocular abnormalities [68]. Both of these studies were conducted on p53-null mice with a C57BL/6 background. Similar ocular abnormalities [68] and attenuated developmental neuronal cell death [43] have not been observed in p53-null mice with a 129/Sv background. The reason for this is unclear, but alleles present in C57BL/6 mice may play a role in influencing the pathway of cell death taken by neurons exposed to different damaging stimuli.

ACKNOWLEDGEMENTS

This work was supported by grants R29 EY12223 (RWN) and R01 EY09091 (AEG) from the National Institutes of Health, the American Health Assistance Foundation, the Retina Research Foundation, the Glaucoma Research Foundation, and Research to Prevent Blindness, Inc.

REFERENCES

1. Buchi ER. Cell death in the rat retina after a pressure-induced ischaemia-reperfusion insult: an electron microscopic study I. Ganglion cell layer and inner nuclear layer. Exp Eye Res 1992; 55:605-13.
2. Buchi ER. Cell death in rat retina after pressure-induced ischaemia-reperfussion insult: electron microscopic study II. Outer nuclear layer. Jpn J Ophthalmol 1992; 36:62-8.
3. Koh JY, Choi DW. Selective blockade of non-NMDA receptors does not block rapidly triggered glutamate-induced neuronal death. Brain Res 1991; 548:318-21.
4. Siliprandi R, Canella R, Carmignoto G, Schiavo N, Zanellato A, Zanoni R, Vantini G. N-methyl-D-aspartate-induced neurotoxicity in the adult rat retina. Vis Neurosci 1992; 8:567-73.
5. Joo CK, Choi JS, Ko HW, Park KY, Sohn S, Chun MH, Oh YJ, Gwag BJ. Necrosis and apoptosis after retinal ischemia: involvement of NMDA-mediated excitotoxicity and p53. Invest Ophthalmol Vis Sci 1999; 40:713-20.
6. Lam TT, Abler AS, Kwong JM, Tso MO. N-methyl-D-aspartate (NMDA)—induced apoptosis in rat retina. Invest Ophthalmol Vis Sci 1999; 40:2391-7.
7. Lipton SA, Rosenberg PA. Excitatory amino acids as a final common pathway for neurologic disorders. N Engl J Med 1994; 330:613-22.
8. Watanabe M, Mishina M, Inoue Y. Differential distributions of the NMDA receptor channel subunit mRNAs in the mouse retina. Brain Res 1994; 634:328-32.
9. Li Y, Schlamp CL, Nickells RW. Experimental induction of retinal ganglion cell death in adult mice. Invest Ophthalmol Vis Sci 1999; 40:1004-8.
10. Schuettauf F, Naskar R, Vorwerk CK, Zurakowski D, Dreyer EB. Ganglion cell loss after optic nerve crush mediated through AMPA-kainate and NMDA receptors. Invest Ophthalmol Vis Sci 2000; 41:4313-6.
11. Otori Y, Wei JY, Barnstable CJ. Neurotoxic effects of low doses of glutamate on purified rat retinal ganglion cells. Invest Ophthalmol Vis Sci 1998; 39:972-81.
12. Mosinger JL, Price MT, Bai HY, Xiao H, Wozniak DF, Olney JW. Blockade of both NMDA and non-NMDA receptors is required for optimal protection against ischemic neuronal degeneration in the in vivo adult mammalian retina. Exp Neurol 1991; 113:10-7.
13. Dreyer EB, Zurakowski D, Schumer RA, Podos SM, Lipton SA. Elevated glutamate levels in the vitreous body of humans and monkeys with glaucoma. Arch Ophthalmol 1996; 114:299-305.
14. Yoles E, Schwartz M. Elevation of intraocular glutamate levels in rats with partial lesion of the optic nerve. Arch Ophthalmol 1998; 116:906-10.
15. Ferrer I, Martin F, Serrano T, Reiriz J, Perez-Navarro E, Alberch J, Macaya A, Planas AM. Both apoptosis and necrosis occur following intrastriatal administration of excitotoxins. Acta

Neuropathol (Berl) 1995; 90:504-10.
16. van Lookeren Campagne M, Lucassen PJ, Vermeulen JP, Balazs R. NMDA and kainate induce internucleosomal DNA cleavage associated with both apoptotic and necrotic cell death in the neonatal rat brain. Eur J Neurosci 1995; 7:1627-40.
17. Ankarcrona M, Dypbukt JM, Bonfoco E, Zhivotovsky B, Orrenius S, Lipton SA, Nicotera P. Glutamate-induced neuronal death: a succession of necrosis or apoptosis depending on mitochondrial function. Neuron 1995; 15:961-73.
18. Bonfoco E, Krainc D, Ankarcrona M, Nicotera P, Lipton SA. Apoptosis and necrosis: two distinct events induced, respectively, by mild and intense insults with N-methyl-D-aspartate of nitric oxide/superoxide in cortical cell cultures. Proc Natl Acad Sci U S A 1995; 92:7162-6.
19. Portera-Cailliau C, Price DL, Martin LJ. Non-NMDA and NMDA receptor-mediated excitotoxic neuronal deaths in adult brain are morphologically distinct: further evidence for an apoptosis-necrosis continuum. J Comp Neurol 1997; 378:88-104.
20. Grilli M, Memo M. Possible role of NF-kappaB and p53 in the glutamate-induced pro-apoptotic neuronal pathway. Cell Death Differ 1999; 6:22-7.
21. Ientile R, Macaione V, Teletta M, Pedale S, Torre V, Macaione S. Apoptosis and necrosis occurring in excitotoxic cell death in isolated chick embryo retina. J Neurochem 2001; 79:71-8.
22. Clarke PG. Developmental cell death: morphological diversity and multiple mechanisms. Anat Embryol (Berl) 1990; 181:195-213.
23. Levine AJ. p53, the cellular gatekeeper for growth and division. Cell 1997; 88:323-31.
24. Miyashita T, Reed JC. Tumor supressor p53 is a direct transcriptional activator of the human bax gene. Cell 1995; 80:293-9.
25. Schlamp CL, Johnson EC, Li Y, Morrison JC, Nickells RW. Changes in Thy1 gene expression associated with damaged retinal ganglion cells. Mol Vis 2001; 7:192-201 .
26. Miller TM, Moulder KL, Knudson CM, Creedon DJ, Deshmukh M, Korsmeyer SJ, Johnson EM Jr. Bax deletion further orders the cell death pathway in cerebellar granule cells and suggests a caspase-independent pathway to cell death. J Cell Biol 1997; 139:205-17.
27. Salvesen GS, Dixit VM. Caspases: intracellular signaling by proteolysis. Cell 1997; 91:443-6.
28. Thornberry NA, Lazebnik Y. Caspases: enemies within. Science 1998; 281:1312-6.
29. Slee EA, Harte MT, Kluck RM, Wolf BB, Casiano CA, Newmeyer DD, Wang HG, Reed JC, Nicholson DW, Alnemri ES, Green DR, Martin SJ. Ordering the cytochrome c-initiated caspase cascade: hierarchical activation of caspases-2, -3, -6, -7, -8, and -10 in a caspase-9-dependent manner. J Cell Biol 1999; 144:281-92.
30. Morrison RS, Wenzel HJ, Kinoshita Y, Robbins CA, Donehower LA, Schwartzkroin PA. Loss of the p53 tumor suppressor gene protects neurons from kainate-induced cell death. J Neurosci 1996; 16:1337-45.
31. Crumrine RC, Thomas AL, Morgan PF. Attenuation of p53 expression protects against focal ischemic damage in transgenic mice. J Cereb Blood Flow Metab 1994; 14:887-91.
32. Rosenbaum DM, Rosenbaum PS, Gupta H, Singh M, Aggarwal A, Hall DH, Roth S, Kessler JA. The role of the p53 protein in the selective vulnerability of the inner retina to transient ischemia. Invest Ophthalmol Vis Sci 1998; 39:2132-9.
33. Jacks T, Remington L, Williams BO, Schmitt EM, Halachmi S, Bronson RT, Weinberg RA. Tumor spectrum analysis in p53-mutant mice. Curr Biol 1994; 4:1-7.
34. Bancroft JD, Stevens A. Bielschowsky's silver stain for axons in frozen and paraffin sections (modified). In: Bancroft JD, Stevens A, editors. Theory and practice of histological techniques. 3rd ed. New York: Churchill Livingstone; 1990. p. 347-8.
35. Chomczynski P, Sacchi N. Single-step method of RNA isolation by acid guanidinium thiocyanate-phenol-chloroform extraction. Anal Biochem 1987; 162:156-9.
36. Schlamp CL, Poulsen GL, Nork TM, Nickells RW. Nuclear exclusion of wild-type p53 in immortalized human retinoblastoma cells. J Natl Cancer Inst 1997; 89:1530-6.
37. Gavrieli Y, Sherman Y, Ben-Sasson SA. Identification of programmed cell death in situ via specific labeling of nuclear DNA fragmentation. J Cell Biol 1992; 119:493-501.
38. Miller FD, Pozniak CD, Walsh GS. Neuronal life and death: an essential role for the p53 family. Cell Death Differ 2000; 7:880-8.
39. Hermann DM, Kilic E, Hata R, Hossmann KA, Mies G. Relationship between metabolic dysfunctions, gene responses and delayed cell death after mild focal cerebral ischemia in mice. Neuroscience 2001; 104:947-55.
40. Culmsee C, Zhu X, Yu QS, Chan SL, Camandola S, Guo Z, Greig NH, Mattson MP. A synthetic inhibitor of p53 protects neurons against death induced by ischemic and excitotoxic insults, and amyloid beta-peptide. J Neurochem 2001; 77:220-8.
41. Copani A, Uberti D, Sortino MA, Bruno V, Nicoletti F, Memo M. Activation of cell-cycle-associated proteins in neuronal death: a mandatory or dispensable path? Trends Neurosci 2001; 24:25-31.
42. Leist M, Jaattela M. Four deaths and a funeral: from caspases to alternative mechanisms. Nat Rev Mol Cell Biol 2001; 2:589-98.
43. Donehower LA, Harvey M, Slagle BL, McArthur MJ, Montgomery CA Jr, Butel JS, Bradley A. Mice deficient for p53 are developmentally normal but susceptible to spontaneous tumours. Nature 1992; 356:215-21.
44. Davies AM, Rosenthal A. Neurons from mouse embryos with a null mutation in the tumour suppressor gene p53 undergo normal cell death in the absence of neurotrophins. Neurosci Lett 1994; 182:112-4.
45. Clarke AR, Purdie CA, Harrison DJ, Morris RG, Bird CC, Hooper ML, Wyllie AH. Thymocyte apoptosis induced by p53-dependent and independent pathways. Nature 1993; 362:849-52.
46. Pan H, Griep AE. Temporally distinct patterns of p53-dependent and p53-independent apoptosis during mouse lens development. Genes Dev 1995; 9:2157-69.
47. Berges RR, Furuya Y, Remington L, English HF, Jacks T, Isaacs JT. Cell proliferation, DNA repair, and p53 function are not required for programmed death of prostatic glandular cells induced by androgen ablation. Proc Natl Acad Sci U S A 1993; 90:8910-4.
48. Hopp RMP, Ransom N, Hilsenbeck SG, Papermaster DS, Windle JJ. Apoptosis in the murine rd1 retinal degeneration is predominantly p53-independent. Mol Vis 1998; 4:5 .
49. Tewari M, Quan LT, O'Rourke K, Desnoyers S, Zeng Z, Beidler DR, Poirier GG, Salvesen GS, Dixit VM. Yama/CPP32 beta, a mammalian homolog of CED-3, is a CrmA-inhibitable protease that cleaves the death substrate poly(ADP-ribose) polymerase. Cell 1995; 81:801-9.
50. Kermer P, Klocker N, Labes M, Bahr M. Inhibition of CPP32-like proteases rescues axotomized retinal ganglion cells from secondary cell death in vivo. J Neurosci 1998; 18:4656-62.
51. Kermer P, Klocker N, Labes M, Thomsen S, Srinivasan A, Bahr M. Activation of caspase-3 in axotomized rat retinal ganglion

cells in vivo. FEBS Lett 1999; 453:361-4.
52. Kermer P, Ankerhold R, Klocker N, Krajewski S, Reed JC, Bahr M. Caspase-9: involvement in secondary death of axotomized rat retinal ganglion cells in vivo. Brain Res Mol Brain Res 2000; 85:144-50.
53. Weise J, Isenmann S, Bahr M. Increased expression and activation of poly(ADP-ribose) polymerase (PARP) contribute to retinal ganglion cell death following rat optic nerve transection. Cell Death Differ 2001; 8:801-7.
54. Katai N, Yoshimura N. Apoptotic retinal neuronal death by ischemia-reperfusion is executed by two distinct caspase family proteases. Invest Ophthalmol Vis Sci 1999; 40:2697-705.
55. Kwong JM, Lam TT. N-methyl-D-aspartate (NMDA) induced apoptosis in adult rabbit retinas. Exp Eye Res 2000; 71:437-44.
56. Deckwerth TL, Elliot JL, Knudson CM, Johnson EM Jr, Snider WD, Korsmeyer SJ. BAX is required for neuronal death after trophic factor deprivation and during development. Neuron 1996; 17:401-11.
57. Ogilvie JM, Deckwerth TL, White FA, Lett JM, Knudson CM, Johnson EM, Snider WD, Korsmeyer SJ. Bax knockout mice have an increased survival of retinal neurons. Invest Ophthalmol Vis Sci 1997; 38:S33.
58. Pastorino JG, Chen ST, Tafani M, Snyder JW, Farber JL. The overexpression of Bax produces cell death upon induction of the mitochondrial permeability transition. J Biol Chem 1998; 273:7770-5.
59. Li Y, Schlamp CL, Poulsen KP, Nickells RW. Bax-dependent and independent pathways of retinal ganglion cell death induced by different damaging stimuli. Exp Eye Res 2000; 71:209-13.
60. Lankiewicz S, Marc Luetjens C, Truc Bui N, Krohn AJ, Poppe M, Cole GM, Saido TC, Prehn JH. Activation of calpain I converts excitotoxic neuron death into a caspase-independent cell death. J Biol Chem 2000; 275:17064-71.
61. Azarian SM, Schlamp CL, Williams DS. Characterization of calpain II in the retina and photoreceptor outer segments. J Cell Sci 1993; 105:787-98.
62. Perrin BJ, Huttenlocher A. Calpain. Int J Biochem Cell Biol 2002; 34:722-5.
63. Mosinger Ogilvie J, Deckwerth TL, Knudson CM, Korsmeyer SJ. Suppression of developmental retinal cell death but not photoreceptor degeneration in Bax-deficient mice. Invest Ophthalmol Vis Sci 1998; 39:1713-20.
64. Chaudhary P, Ahmed F, Quebada P, Sharma SC. Caspase inhibitors block the retinal ganglion cell death following optic nerve transection. Brain Res Mol Brain Res 1999; 67:36-45.
65. Nickells RW. Retinal ganglion cell death in glaucoma: the how, the why, and the maybe. J Glaucoma 1996; 5:345-56.
66. Nickells RW. Apoptosis of retinal ganglion cells in glaucoma: an update of the molecular pathways involved in cell death. Surv Ophthalmol 1999; 43:S151-61.
67. Aloyz RS, Bamji SX, Pozniak CD, Toma JG, Atwal J, Kaplan DR, Miller FD. p53 is essential for developmental neuron death as regulated by the TrkA and p75 neurotrophin receptors. J Cell Biol 1998; 143:1691-703.
68. Ikeda S, Hawes NL, Chang B, Avery CS, Smith RS, Nishina PM. Severe ocular abnormalities in C57BL/6 but not 129/Sv p53-deficient mice. Invest Ophthalmol Vis Sci 1999; 40:1874-8.

The print version of this article was created on 15 Sep 2002. This reflects all typographical corrections and errata to the article through that date. Details of any changes may be found in the online version of the article.